Available at
www.ElsevierComputerScience.com
POWERED BY SCIENCE DIRECT®

Medical Image Analysis 8 (2004) 3–22

MEDICAL IMAGE ANALYSIS

www.elsevier.com/locate/media

A deformable digital brain atlas system according to Talairach and Tournoux

Klaus A. Ganser [a,*], Hartmut Dickhaus [a], Roland Metzner [b], Christian R. Wirtz [b]

[a] Department of Medical Informatics, University of Heidelberg, University of Applied Sciences, Max-Planck-Str. 39, D-74081 Heilbronn, Germany
[b] Department of Neurosurgery, University of Heidelberg, Im Neuenheimer Feld 400, D-69120 Heidelberg, Germany

Received 17 June 2002; received in revised form 29 January 2003; accepted 25 June 2003

Abstract

Brain atlases are valuable tools which assist neurosurgeons during the planning of an intervention. Since a printed atlas book has several disadvantages – among them the difficulty to map the information onto a patient's individual anatomy – we have developed a digital version of the well-established stereotaxic brain atlas of Talairach and Tournoux. Our atlas system is mainly dedicated to assist neurosurgical planning, and its benefits are: (i) a three-dimensional (3D) representation of most brain structures contained in the Talairach atlas; (ii) a nonrigid matching capability which warps the standard atlas anatomy to an individual brain magnetic resonance imaging (MRI) dataset in a few minutes and which is able to take deformations due to tumors into account; (iii) the integration of several sources of neuroanatomical knowledge; (iv) an interface to a navigation system which allows utilization of atlas information intraoperatively. In this paper we outline the algorithm we have developed to achieve 3D surface models of the brain structures. Moreover, we describe the nonrigid matching method which consists of two tasks: firstly, point correspondences between the atlas and the patient are established in an automatic fashion, and secondly these displacement vectors are interpolated using a radial basis function approach to form a continuous transformation function. To generate appropriate target structures for the first of these tasks, we implemented a quick segmentation tool which is capable to segment the cortex and ventricles in less than 5 min. An evaluation shows that our nonrigid approach is more precise than the conventional piecewise linear matching, though it should be further improved for the region around the deep grey nuclei. Summarizing, we developed a Win32 program which permits the convenient and fast application of standardized anatomy to individual brains which potentially contain tumors.

Keywords: Brain atlas; Nonrigid atlas matching; Neurosurgical planning

1. Introduction

Neurosurgical interventions have to be carefully planned with high precision to allow maximally sparing trajectories to brain lesions (Kelly, 1996). All frequently used imaging modalities, especially magnetic resonance imaging (MRI), support the physician in identifying important structures in the brain and bearing them in mind for the surgical strategy. However, many of the brain structures are hardly or not at all visible in the acquired images. Therefore, neurosurgeons frequently consult brain atlases during the planning of interventions to improve their orientation. Brain atlases are usually printed books (the most well known are those of Schaltenbrand and Wahren (1977) and Talairach and Tournoux (1988)), which makes their application to patient's images tedious and often erroneous. Because there are differences between an atlas book and a MR image concerning dimensionality (2D plates versus 3D volume dataset), medium of representation (printed on paper versus digital display), and anatomic shape (standard anatomy versus individual brain), the information transfer from the atlas to the MR image has to happen solely in the mind of the surgeon. It is evident that this procedure stresses the physician's 3D imaginative capability very much, and it requires a long time experience to gain success. The usage of a book in the aseptic environment

* Corresponding author.
E-mail address: ganser@fh-heilbronn.de (K.A. Ganser).

1361-8415/$ - see front matter © 2003 Elsevier B.V. All rights reserved.
doi:10.1016/j.media.2003.06.001

of the operating theatre is an additional problem which limits the application of an atlas to the preoperative planning stage. An other disadvantage of a printed atlas book is its finality, i.e. there is no way to correct errors and include new insights or further information.

To overcome these problems, as neurosurgeons demand, we decided to develop a computerized atlas system. As anatomic basis we chose the well-established stereotaxic brain atlas of Talairach and Tournoux (1988), although we know that the Talairach atlas itself has several disadvantages: it is two-dimensional (2D), is relatively sparse due to inter-slice distances of 2–5 mm, assumes left/right symmetry, and contains some inconsistencies between orthogonal plates. However, one can not neglect the fact that it is actually used by many neurosurgical groups for planning of interventions. Certainly this is the reason why in the past several working groups have built computerized atlas systems around the Talairach atlas. But, as we will discuss later, all systems proposed so far have some shortcomings.

We state a list of requirements which our computerized atlas system should fulfill in order to overcome the disadvantages of printed atlas books as well as those of the Talairach atlas and those of other existing systems:

- It shall include 3D reconstructed surface models of brain structures as well as the original atlas plates,
- it shall provide an easy-to-handle matching feature to adapt the atlas nonrigidly to individual brain images,
- it shall offer a powerful visualization to display atlas and MRI in joint views,
- it shall include additional information which extends the contents of the Talairach atlas; moreover it shall be open to further extensions, and
- it shall offer an interface to a navigation system in order to provide the atlas information intraoperatively.

Our paper is organized as follows. In Section 2 we give a short survey over related work. After this, we present the methods we applied for developing a computerized atlas system in Section 3. In particular, we discuss our 3D reconstruction algorithm (Section 3.1) as well as all the methods necessary for achieving nonrigid matching (Section 3.2). In Section 4, we describe the computerized Talairach atlas system which we developed in respect to accuracy considerations as well as to some application cases. Finally, we discuss the whole development in Section 5, where we also outline further extensions.

2. Related work

Many groups work on the development of computerized brain atlases. Several reports on atlases based on proprietary sources of anatomic knowledge have been published in the last decade: the *Computerized Brain Atlas* (*CBA*) of Thurfjell et al. (1995), the *Montreal Brain Atlas* of Evans et al. (1994), or the atlas of the *International Consortium for Brain Mapping* (*ICBM*) (Mazziotta et al., 2001) are prominent examples. These systems contain probabilistic information on brain anatomy and function originated in large numbers of brains included (up to 7000 in the ICBM case), and can be nonrigidly registered with images of patients. The main focus of these systems is brain mapping rather than surgical planning.

Besides these atlases, the brain atlas of Talairach and Tournoux (1988) was examined frequently since its publication in 1988 (Barillot et al., 1990; Davatzikos et al., 1996; Fang et al., 1995; Lemoine et al., 1991; Migneco et al., 1994; Ou et al., 1998; Schiemann et al., 1994; Garlatti and Sharples, 1998; Chunguang et al., 1998; Nielsen and Hansen, 1998). However, the majority of these systems only uses the 2D atlas plates, which have been simply scanned in (Barillot et al., 1990; Davatzikos et al., 1996; Lemoine et al., 1991; Migneco et al., 1994; Ou et al., 1998; Schiemann et al., 1994; Nielsen and Hansen, 1998). Because the distance between adjacent maps in the Talairach atlas is unpleasently large (2–5 mm), these systems suffer from wide gaps where no atlas information is available, and furthermore the difference in dimensionality still exists. Some of the proposed systems present atlas plates and MR images side by side (Barillot et al., 1990; Lemoine et al., 1991; Schiemann et al., 1994), which however is not a sufficient solution to the transfer problem mentioned above. The goal of some of the proposed systems is in the field of computer based training of neuroanatomy (Garlatti and Sharples, 1998; Chunguang et al., 1998), so they do not focus on mapping the atlas to patients' brains. Most of the other systems use the proportional grid, Talairach's brain coordinate frame, for a piecewise linear matching procedure. This matching paradigm performs well for structures located near the brain stem and for datasets not affected by deforming pathologies. However, for the cortex or in presence of large tumors the proportional grid model is too simple. Davatzikos et al. (1996) are the first to introduce a nonrigid registration algorithm for Talairach atlas plates, but this approach still works in 2D. In another publication from this group dating to the same year (Davatzikos, 1996) a general purpose 3D matching algorithm is described. One of the presented examples uses a stack of 2D Talairach atlas plates as one modality; however the algorithm matches the MR dataset onto the atlas, i.e. the atlas keeps unchanged while the MR dataset gets warped appropriately. However, for surgical planning it is much more reasonable to perform the matching in the opposite direction. Kyriacou et al. (1999) use a 2D finite element model of an axial atlas plate for an elastic matching. They present an

example where they are able to simulate tumor growth in the atlas anatomy.

The most advanced computerized Talairach atlas system so far was developed at the Kent Ridge Digital Laboratories, Singapore (Fang et al., 1995; Nowinski et al., 1997). They realized a fully 3D reconstruction of the atlas and included it into a powerful "brain bench", a system which contains several brain atlases and provides piecewise linear matching with clinical images. A very recent work of this group focuses on a nonrigid matching procedure based on the finite element method (Xu and Nowinski, 2001).

A somewhat different application built around the Talairach atlas is the so-called Talairach Daemon developed by Lancaster et al. (2000). The Daemon is a database which contains hierarchically structured anatomical knowledge for each coordinate in the Talairach frame, as well as statistical maps which indicate probabilities for brain structures to be located at certain positions. The scope of this database mainly lies in the field of brain mapping.

The Talairach atlas (especially its coordinate system, the proportional grid) often is used in the context of brain normalization, because locations of activations acquired by means of functional MRI are usually described in this coordinate frame. Software like SPM [1] (developed at the University College, London, UK) is dedicated to this task. As in the paper of Davatzikos (1996) (see above) the dataset under consideration is warped towards the atlas. For further information on brain normalization applications see the survey of Lancaster and Fox (2000).

The atlas system we have developed uses the well-established standard anatomy of the Talairach atlas, and is designed to overcome the drawbacks of most of the Talairach systems described above. Our 3D reconstruction approach follows the formulation of Fang et al. (1995), but we have improved their technique in several aspects as it is outlined in Section 3.1. In addition to a linear and a piecewise linear matching capability we have developed a nonrigid registration algorithm utilizing radial basis functions. Our method has several advantages over the one proposed by Xu and Nowinski (2001), among them the ability to cope with deformations due to tumors (compare Section 3.2). To provide the nonrigid registration with appropriate target structures, we implemented very fast segmentation tools for the cortex and the ventricular system; to our knowledge, no other Talairach systems can feature this. Finally, our system offers a variety of visualization options, which allow a convenient recognition of neuroanatomic circumstances in the brain of the patient.

[1] http://www.fil.ion.ucl.ac.uk/spm.

3. Methodological approach

3.1. Three-dimensional reconstruction of atlas structures

The printed atlas book of Talairach and Tournoux (1988) consists of three orthogonal stacks of 2D cross-sections through a brain, which are oriented sagittally, coronally and axially. The inter-slice distance is 2–5 mm. Because surgeons often have to consider 3D brain structures and fibre connections between them, we calculated a 3D reconstruction of all objects contained in the atlas at their appropriate location.

For our work we used only the coronal plates. After scanning the 38 plates with a resolution of 0.2 mm per pixel we segmented them interactively and labelled 49 different anatomical objects (e.g. ventricles, thalamus, putamen, etc.). We obtain slices only containing the unambiguously labelled structures; the acronyms, numbers and coordinate axes have been removed. Then we improved the spatial resolution by interpolating additional cross-sections between each pair of adjacent original plates. To interpolate the shape of an object for the new cross-section, we calculated a Delauney tetrahedrization of the object using the Nuages algorithm proposed by Geiger (1993). The shell surface of the resulting solid was then intersected at half the slice distance. The stacked original and interpolated slices can be considered as a binary voxel space, where the grey value of each voxel indicates the structure the voxel belongs to. We achieve a smoothing of the terraced shapes by applying a spatial low pass convolution filter (a 9×9 Gaussian filter with $\sigma = \sqrt{2}$ pixels in-plane, and calculating the mean of two adjacent slices). Thereafter we extract the surface representation of the objects with the marching cubes algorithm (Lorensen and Cline, 1987). We decimated the enormous amount of surface triangles produced by this method by applying the polygon reduction algorithm proposed by Melax (1998). The number of vertices was reduced this way to 50% without noticeable loss of quality (compare Fig. 2(d)).

The lateral symmetry of the brain gives rise to a high redundancy in brain cross-sections, for which reason Talairach and Tournoux only drew one hemisphere in detail. We exploited this symmetry for further reduction of data as well: we only process the right hemisphere of the atlas and mirror it at the midsagittal plane to the left side. In Fig. 1 we summarize the image processing steps which we performed to achieve the 3D reconstruction. The result of the reconstruction algorithm is demonstrated in Fig. 2 by example of the lateral ventricles.

3.2. Matching of atlas and MR datasets

3.2.1. Segmentation of cortex and ventricles

We have implemented a segmentation tool in our atlas system by which a 3D representation of the cortex

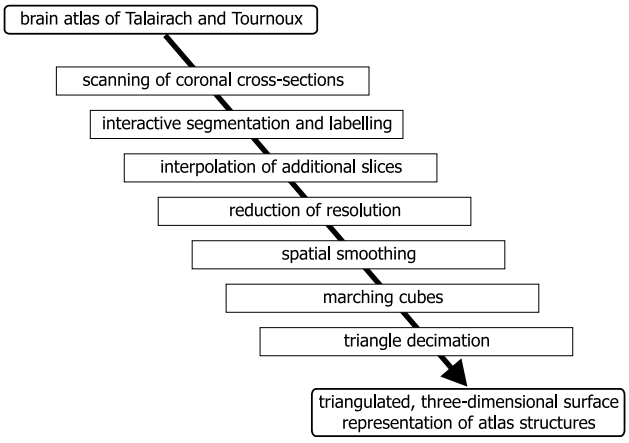

Fig. 1. The sequence of image processing operations performed for three-dimensional reconstruction of the Talairach atlas structures.

and ventricles can be achieved. The development is motivated by two reasons: (i) The common presentation of the patient's anatomy by means of three orthogonal cross-sections through the MRI stack is quite useful, but still lacks a real 3D-impression. A segmented structure can easily be visualized in 3D and thus can grant a very intuitive impression. (ii) We need well-defined structures which can be used to direct the nonrigid matching process described below. A segment demarcates objects uniquely and that way can serve as a target structure.

We assess the grey value histogram of the dataset, where the user has to select two thresholds enclosing the grey value range of the brain tissue. After binarizing the image stack with these thresholds, morphological operators like erosion, dilation and selection (this means finding and conserving the biggest connected component while rejecting all smaller ones), as well as median filtering and drawing routines are available as postprocessing tools. We figured out a sequence of operations – erosion, median filtering, selection, dilation – which in most cases immediately leads to the final segmentation. A similar segmentation framework has been proposed earlier by Höhne and Hanson (1992). An additional

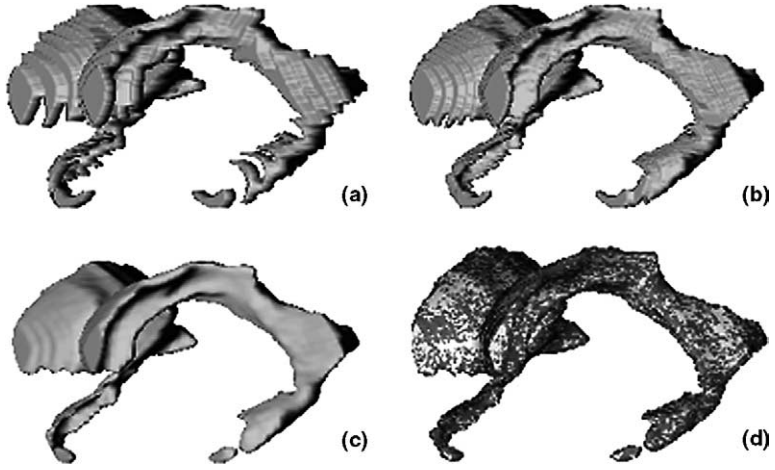

Fig. 2. Increasing quality of reconstruction corresponding with different steps of our algorithm. The effects are demonstrated on the lateral ventricles. (a) The marching cubes algorithm was applied before additional interpolation. Obviously the result has little in common with the real ventricles. (b) Additional slices have been interpolated. A more realistic shape appears. (c) Spatial smoothing of the interpolated structures has been performed. A nice, realistic appearance of the ventricles is achieved (note that, unfortunately, the most frontal part of the inferior horn got detached by the spatial smoothing). (d) Comparison of the full (dark) and the decimated (light) surface model by means of simultaneous visualization. Obviously both shapes are nearly identical; the differences between them are very small and rather stochastic.

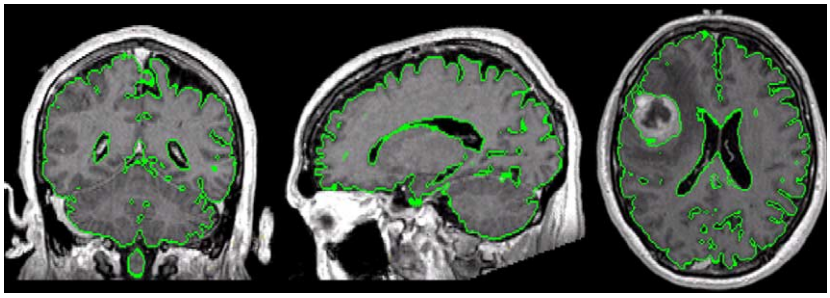

Fig. 3. Three orthogonal cuts through a patient's MR dataset; the contour line of the brain segment acquired with the segmentation algorithm described in Section 3.2.1 are overlayed in green, which allows for assessing the quality of the segmentation. Note that the tumor does not belong to the segment due to the higher grey values in its outer part, which do not fit into the brain's grey value range and which shield and separate the inner part from the segment. However this is not a problem because we are only interested in the overall shape of the cortex, which is complete. (This figure is available in colour, see the on-line version.)

segmentation tool is a region grower we implemented in the system. Visual control is granted after each operation. In Fig. 3 the quality of the segmentation can be judged on three orthogonal MR cross-sections containing overlayed segment contours. With the described toolset the segmentation of the cortex lasts less than 5 min in most cases, which makes the system attractive for clinical routine use. In Figs. 4(a) and (e) examples of a segmented cortex and segmented ventricles can be seen in a 3D visualization.

3.2.2. Tagging of tumors and sulci

For the same reasons for which we implemented the segmentation features, we developed tools for drawing simple structures in the scene. These tools are especially suited for tagging of tumors and sulci. The functionality of the tool includes convenient insertion, deletion and movement of vertices as it is commonly known from commercial graphics software. Three-dimensional reconstructions from stacks of drawn polygons can be calculated with the Nuages algorithm (Geiger, 1993). The tumor segment visible in Fig. 4(i) was constructed with this tool as well as the electrodes displayed in Fig. 14.

Tagging of sulci on the cortex segment would be difficult, because, as we will explain in Section 3.2.5, the resulting line is expected to lay on the cortex's envelope. To be able to tag a sulcus in this way, we perform morphological closing on the cortex segment and use the set difference between the closed and the original cortex to fill the sulcus concavities. On these inlays the user can easily draw the sulcus line.

3.2.3. Piecewise linear matching of atlas and MR images

The Talairach atlas is drawn in a proportional coordinate system, the so called "proportional grid", which can be adapted piecewise linearly to individual brain geometries. It is based on the anterior and the posterior commissures (CA and CP) and on the maximal extent of the brain in three orthogonal directions.

Our computerized atlas can be matched to MR images of patients by means of this proportional grid. The MRI dataset is displayed in three orthogonal cross-sections – coronal, axial and sagittal. In this scene we insert the proportional grid as a wireframe model. The grid has to be adjusted interactively by means of translation, rotation and piecewise scaling, until the nodes of the grid coincide with the landmarks CA and CP and with the size of the brain in the MRI. During this task, the entire scene can be rotated and zoomed as well to find the best point of view to judge the conformity of the

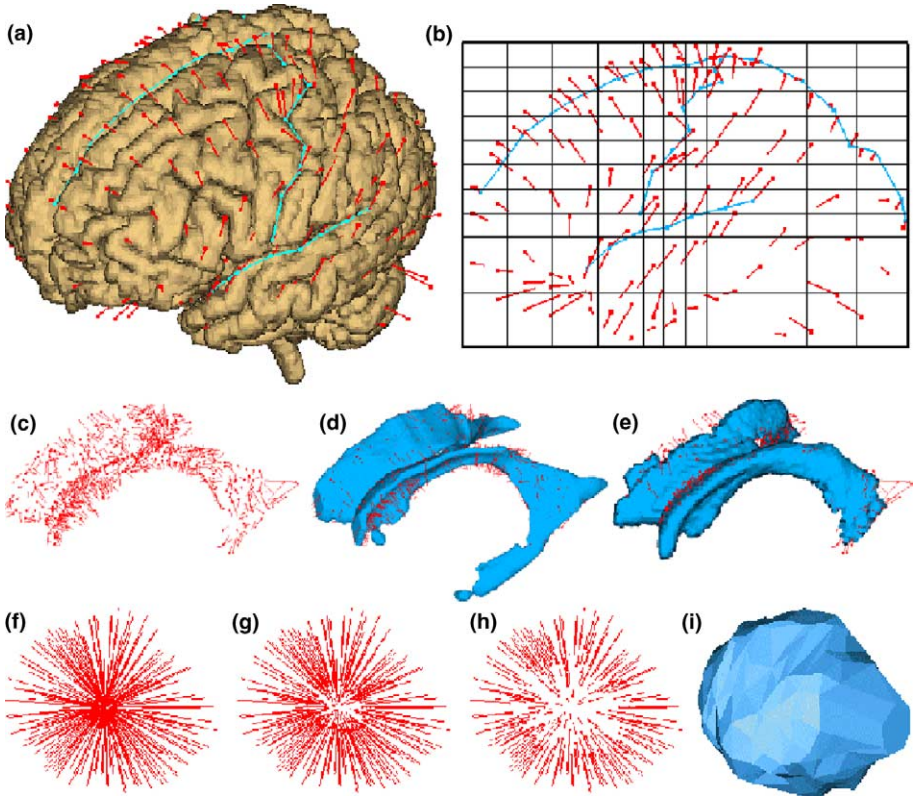

Fig. 4. Displacement vectors generated by our algorithms. (a) Vectors (red) found at the cortex; the influence of several sulci (s. centralis, s. lateralis, s. longitudinalis, displayed in blue) is obvious. (b) Same situation as (a) in a projective view from the left. In black the proportional grid is overlayed. (c) Vectors found at the lateral ventricles. These vectors are displayed in the context of the atlas ventricles (d) and the patient ventricles (e). (f) Vectors constructed for a tumor with shrinkage to 10% respectively 30% (g) and 60% (h). In (i) a surface visualization of the tumor is shown. (This figure is available in colour, see the on-line version.)

landmark locations. The MRI dataset is afterwards transformed rigidly (rotation and translation) into the coordinate system of the atlas. Trilinear interpolation is used for this transformation. The atlas is then matched to the extent of the brain under consideration by means of the piecewise affine deformation.

The proportional grid matching is used for a global preregistration of atlas and MR datasets. For the following steps aiming to nonrigid matching we therefore can presume a rough congruence between the atlas and the patient's brain.

3.2.4. Nonrigid matching using Radial basis functions

Besides the common matching approach outlined in the previous section, we developed a nonrigid matching algorithm to improve the concordance. It utilizes radial basis functions, a method known from interpolation theory, which can be adopted for interpolating displacement vectors. Thus we have to find point correspondences between atlas and patient, and by interpolating them throughout the image continuum, we get a transformation function $\mathscr{T}:\mathbb{R}^3\to\mathbb{R}^3$ which maps the atlas onto the patient's brain. Of course the mapping has to be considered as an estimate for the location in patient space where each atlas point may be assumed to be located. For now we assume the displacement vectors as given; in Section 3.2.5 we will describe how we actually determine these point correspondences.

In the following we will denote a point of the atlas as $\vec{a}$ and a point of the patient as $\vec{p}$. Given a set of N point correspondences $(\vec{a}_i,\vec{p}_i)$ with $i\in\{1,2,\ldots,N\}$, we are looking for a transformation function $\mathscr{T}:\mathbb{R}^3\to\mathbb{R}^3$ which satisfies the interpolation condition $\mathscr{T}(\vec{a}_i)=\vec{p}_i$. The function $\mathscr{T}$ is a radial basis function transformation, which is defined as

$$\mathscr{T}(\vec{a})=\mathscr{A}(\vec{a})+\mathscr{R}(\vec{a}), \tag{1}$$

where $\mathscr{A}$ is an affine mapping and $\mathscr{R}$ is a radial transformation. For $\mathscr{A}$ we write

$$\mathscr{A}(\vec{a})=(\mathscr{A}_x(\vec{a}),\mathscr{A}_y(\vec{a}),\mathscr{A}_z(\vec{a}))^{\mathrm{T}},$$

where

$$\mathscr{A}_k(\vec{a})=\alpha_{k,1}+\alpha_{k,2}\cdot a_x+\alpha_{k,3}\cdot a_y+\alpha_{k,4}\cdot a_z,\quad k\in\{x,y,z\}. \tag{2}$$

The radial transformation $\mathscr{R}$ can be similarly distributed to

$$\mathscr{R}(\vec{a})=(\mathscr{R}_x(\vec{a}),\mathscr{R}_y(\vec{a}),\mathscr{R}_z(\vec{a}))^{\mathrm{T}},$$

where

$$\mathscr{R}_k(\vec{a})=\sum_{i=1}^{N}\beta_{k,i}\cdot r(|\vec{a}-\vec{a}_i|),\quad k\in\{x,y,z\}. \tag{3}$$

The function $r:\mathbb{R}_0^+\to\mathbb{R}$ is the radial basis function; it is solely dependent on the euclidean distance $|\cdot|$ of an arbitrary point $\vec{a}$ in atlas space to the given atlas points $\vec{a}_i$. Altogether, $\mathscr{T}$ is determined by $3\cdot(N+4)$ unknown coefficients, $N+4$ in each of the coordinates $k\in\{x,y,z\}$. To find the coefficients in each dimension, a linear equation system of size $N+4$ has to be solved. The N coefficients $\beta_{k,i}$ are constituted by the given point correspondences $(\vec{a}_i,\vec{p}_i)$, while for the four coefficients $\alpha_{k,j}$ additional constraints have to be stated. A common approach is to use a normalization as

$$\sum_{i=1}^{N}\beta_{k,i}=0,\quad \sum_{i=1}^{N}\beta_{k,i}a_{i,x}=0,$$
$$\sum_{i=1}^{N}\beta_{k,i}a_{i,y}=0,\quad \sum_{i=1}^{N}\beta_{k,i}a_{i,z}=0.$$

Therefore, the linear equation system can be written as

$$\begin{pmatrix}\boldsymbol{R} & \boldsymbol{A}\\ \boldsymbol{A}^{\mathrm{T}} & \boldsymbol{0}\end{pmatrix}\begin{pmatrix}\overrightarrow{\beta_k}\\ \overrightarrow{\alpha_k}\end{pmatrix}=\begin{pmatrix}\vec{P}_k\\ \vec{0}\end{pmatrix},\quad k\in\{x,y,z\}. \tag{4}$$

From Eqs. (2) and (3) the entries of the $N\times N$ submatrix $\boldsymbol{R}$ and of the $N\times 4$ submatrix $\boldsymbol{A}$ can be determined; the $N\times 1$ vector $\vec{P}_k$ contains the kth dimension of the N target points $\vec{p}_i$: it holds $P_{k,i}=p_{i,k}$. Obviously, the matrix in Eq. (4) is independent from the dimension k, for which reason it needs to be built only once for all three cases $k\in\{x,y,z\}$.

In the literature a variety of different radial basis functions r are described (see e.g. Fornefett et al., 2001; Arad and Reisfeld, 1995); presumably the most well known is the Thin Plate Spline, which is defined as $r_{\mathrm{TPS}}(d)=d^2\ln d^2$ for $d>0$ and 0 for $d=0$. We have implemented several of these in our atlas system. We achieved best results concerning runtime and quality of mapping with the $\psi_{3,0}$-function of Wendland (1998) (see also Fornefett et al., 2001), which is defined by $r_{\psi_{3,0}}(d)=(1-d/\gamma)^2$ for $0\leqslant d\leqslant\gamma$, and 0 elsewhere (the locality parameter γ is set to a value of 40 mm). For this reason we exclusively use this basis function in practice.

3.2.5. Determination of point correspondences

In the previous section we described how we calculate an interpolation of given point correspondences. Here we present the methods we apply for actually determining these pairs of corresponding points. Because the brain anatomy is rather complex, as much point correspondences as possible should be taken into account. We have developed methods to construct displacement vectors at the cortex (thereby regarding the major sulci), at the lateral ventricles, and at the commissures. Moreover, we introduce vectors in the vicinity of tumors to model their space-occupying behaviour in the transformation function.

Cortex: The method for finding point correspondences on the cortex is divided into two steps. The first one only considers the major sulci which the user has tagged in the patient's brain and which, of course, are known in the atlas (the term "sulcus" here refers to the

visible part of a sulcus, a line in 3D space which roughly is the projection of the furrow to the envelope of the cortex). Normalizing the length of these sulcus lines of each atlas and patient leads to parametric functions $\mathscr{S}_{\text{atlas}}(t)$ and $\mathscr{S}_{\text{patient}}(t)$ defined over the unity interval. Point correspondences are given implicitly by the mapping $\mathscr{S}_{\text{atlas}}(t) \mapsto \mathscr{S}_{\text{patient}}(t)$ for $0 \leqslant t \leqslant 1$. Having established correspondences at the central sulcus, the sylvian and the longitudinal fissure, we use the radial basis function approach to interpolate this set of displacement vectors to a transformation function.

For the second step, the system knows about 200 points on the atlas cortex, all lying on top of gyri and therefore on the envelope of the cortex. We apply the transformation function from the first step to these, which results in a redistribution of the atlas cortex points. The new point locations inherently consider the given sulcal correspondences. Starting at the new locations, we search for the nearest point on the patient's cortex in a radial direction towards the brain's centre of gravity. We use a morphologically closed cortex segment to be sure to get no points lying inside of sulci.

Ventricles: To determine correspondences at the lateral ventricle, we consider a set of points on the atlas ventricle surface. For each of these points, the nearest point on the patient's ventricle is found in the following way: We calculate a distance transform of the patient ventricle segment (Chamfer-3-4-5 distance metric as proposed by Borgefors, 1984), and we move the atlas start points step by step each in the direction of the steepest descent of the gradient in the distance map. The algorithm converges quickly to the ventricle surface of the patient. It is necessary to check the resulting vectors for plausibility, because a lot of incorrect assignments occur. The difficulty in recognising these is, that we can not assume anything about the shape of the target structure (segmented patient ventricles). There are cases where e.g. the lower horns are not present, or where there is no ventricle at all in one hemisphere, or where the patient's ventricles are much bigger or smaller than the atlas ventricles. In such cases, not only solitary vectors, which could be identified due to their difference to neighbouring vectors, will be wrong. So we have to decide for each single vector whether it is erroneous or not, and we must not take its neighbouring vectors into account for the decision. We apply the following rules, which are motivated geometrically and which are easy to calculate:

- Frequently, wrong displacement vectors are longer than the regular ones; therefore, we use a threshold for the vector length which defaults to 20 mm.
- The normal vectors on the ventricle surface of the atlas (at the start point) and of the patient (at the destination point) must not differ too much. We exclude all displacement vectors for which the angular difference between these normals is greater than 90°.
- We exclude vectors crossing the midsagittal plane.
- Because of the discrete nature of the distance map and the patient's ventricle segment, often more than one atlas point is mapped to the same patient point. Since this is not tolerable, we only conserve the shortest of these displacement vectors and delete the others.

The described algorithm leads to about 600 point correspondences for the ventricular system.

Commissures: The atlas and the MRI dataset have undergone a matching according to the proportional grid. Therefore, the anterior and the posterior commissure can be regarded as coincident, for which reason the loci of the commissures can serve as fixpoints in the nonrigid transformation. We attach displacement vectors of length 0 at these coordinates to fix the points.

Tumors: We assume tumor growth to be directed approximately radially starting from a point-shaped object. Under this assumption, we have to define vectors which blow up a small volume to the shape of the tumor the user has marked (see above). To achieve this, we virtually shrink the tagged tumor to a fraction of its original size and insert displacement vectors between the shrinked and the unshrinked model. Depending on the behaviour of the considered tumor concerning infiltration versus squeezing, the shrink factor can be adjusted. The shrinking should be the less the more infiltrating the tumor behaves. For the described task, 50–100 vectors are needed.

Fig. 4 illustrates the results of the described algorithms.

4. Results

4.1. Design and implementation of an atlas system

In the previous sections we described some methodological basics on 3D reconstruction of the printed Talairach atlas as well as on matching the atlas with MR images of a patient. We used these methods to develop a computerized brain atlas system.

Because all MR scanners supply their images in the DICOM file format, we implemented an import filter for DICOM files. Therefore, the images can be read directly without the necessity of a prior format conversion. A limitation of the import filter is that, in its current implementation, it is only able to read axially sliced datasets with a matrix size of 256×256. To be still able to handle non-DICOM image data from other sources, we offer a raw data import capability, too.

After the matching process – piecewise affine as well as nonrigid – , our system offers several options to display the contents of the atlas together with the MR images. In a 3D scene consisting of three arbitrarily locatable sagittal, coronal and axial MR cross-sections,

the 3D reconstructed atlas objects can be optionally inserted. If an object is cut by a MR cross-section, its contour line can be indicated on the grey value image. Furthermore, the scanned atlas plates with all their useful additional information can be inserted transparently at their appropriate location. All viewing options are available simultaneously; it is possible to display the atlas in its warped as well as in its original shape. The warping influences the 3D reconstructed objects as well as the atlas plates and the wire frame model of the proportional grid. Fig. 5 gives an impression of the various display facilities our system provides.

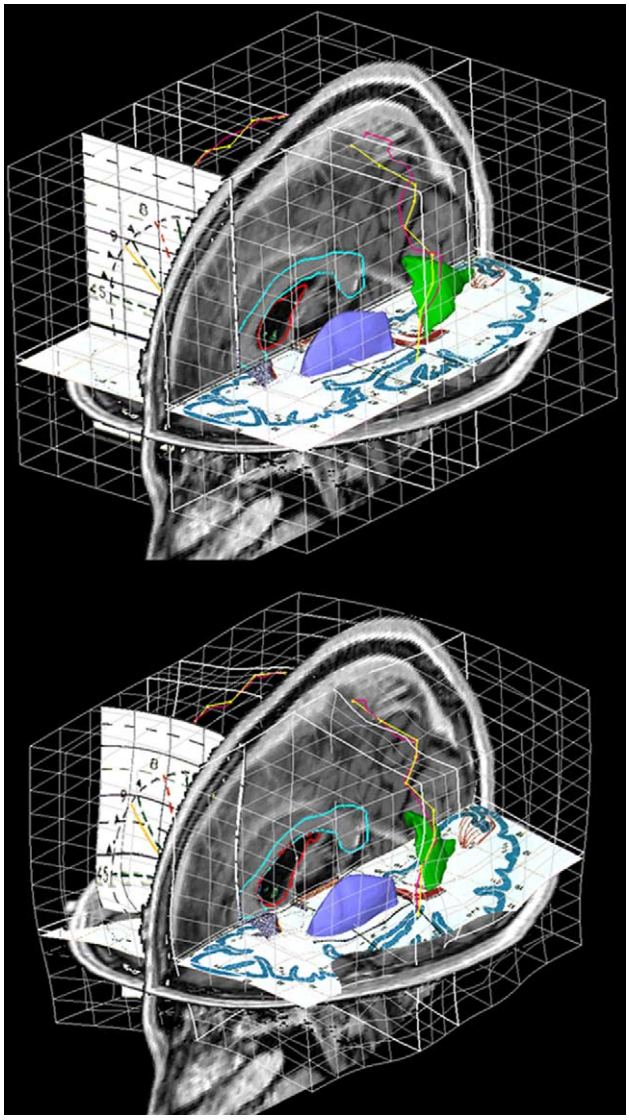

Fig. 5. Several information entities of the digital Talairach atlas displayed in the context of a patient's MRI dataset. Top: situation after piecewise linear matching; bottom: situation after nonrigid matching. Two surface models are visible: putamen (blue) and tapetum (green). Object contours of the lateral ventricles (red loop) and the corpus callosum (cyan loop) are drawn on the sagittal MR cross-section. Two atlas plates (the axial one taken from the Talairach and Tournoux, 1988 atlas, the coronal one from the Talairach and Tournoux, 1993 atlas) and the proportional grid are displayed, too. (This figure is available in colour, see the on-line version.)

Our atlas system includes an interface to a neuronavigation system developed in our department (MOPS-3D by Dickhaus et al., 2002), which is able to cooperate with the tracking systems Polaris (NDI, Waterloo, CA) and Flashpoint (Stryker, Calamazoo, USA). The atlas structures can be saved in a well-defined file format after the performance of the matching procedure. MOPS-3D is able to import these files and to display the structures at their appropriate location. Therefore, the surgeon can recall the location of the standard anatomy during surgery.

Besides the features mentioned so far, our system has some additional useful properties. Among them are: accurate measurement of distances, angles and volumes; the ability to make annotations in the scene; a tool to read out and display the DICOM header information; the ability to read and display overlay data volumes (this feature can be used to display activation spots of fMRI acquisitions, for example); an export filter to save the MR images as Windows bitmap files. It is needless to say that the outcome of all interactive steps (segmentation, matching, measurements, etc.) may be saved and recalled later on.

The following two subsections are dedicated to some special aspects of our development. Firstly we discuss the temporal performance, and secondly we report about additional neurological information we digitally added to our atlas system.

4.1.1. Temporal performance

The runtime and operating performance of our system has been evaluated. A typical application case consists of the following steps: 1. Loading of the patient's image; 2. Adaptation of the proportional grid; 3. Segmentation of the cortex; 4. Segmentation of the ventricles; 5. Tagging of tumor(s) and sulci; 6. Establishing of point correspondences atlas $\leftrightarrow$ patient; 7. Calculation of the nonrigid transformation function; 8. Application of the transformation function to the atlas. Steps 2, 3, 4 and 5 require user interactions, in step 6 the user may exert influence on the final result. A list of typical time requirements for the different tasks, with added comments on the respective circumstances, is given in Table 1. Altogether, in less than half an hour a planning procedure can be completed.

4.1.2. Inclusion of additional information

Every brain atlas can represent only a certain subset of the overwhelming amount of information available on the brain. Using printed atlas books, one has to consult further books if special information is not available in the atlas, which means that a mental mapping procedure has to happen again. In computerized brain atlas systems, it is possible to offer information from several sources with a single mapping, once the

Table 1
Amount of time needed for the steps involved in the application of the atlas system

Step	Time	Comment
1. Loading of patient's image	3 s	For a dataset consisting of 130 DICOM images
2. Adaptation of proportional grid	3 min	Slightly longer for complicated cases (e.g. intraoperative images); including rigid transformation of the MR dataset using tri-linear interpolation
3. Cortex segmentation	30 s	Without the necessity to apply the drawing tools (usually the case)
	5 min	If drawing interactions are necessary
4. Ventricle segmentation	5 min	Absolutely maximum, even in poor images
5. Tumor and Sulci tagging	5 min	Maximum; time is dependent on the tumor size
6. Establishing of point correspondences	2 min	Including the time for control by the user
7. Calc. nonrigid transformation	31 s	Average value; maximum 49 s for a case with a large tumor
8. Apply nonrigid transformation	5 s	Maximum response time (warping of the surface model of the lateral ventricles)

The CPU times (steps 3a, 6, 7, 8) apply for a Intel Celeron 850 MHz, the interaction times (steps 2, 3, 4, 5) for an experienced user.

developer of the system has put the different informations in a unique frame of reference.

We included two sources of visual neurological information: The somatosensoric and motoric homunculi of Penfield and Rasmussen (1950), and the "Referentially Oriented Cerebral MRI Anatomy" by Talairach and Tournoux (1993). Since the rough location of the central sulcus is relatively constant with respect to the proportional grid, the homunculus plates can be positioned automatically with sufficient fidelity. The plates of the second Talairach atlas, containing basal ganglia and fascicles, are likewise drawn in the proportional grid, for which reason an insertion is straight forward. Fig. 5 displays (among other things) one plate from the "Referentially Oriented Cerebral MRI Anatomy". The homunculi are shown in Fig. 6, which also gives an impression of the transparency features.

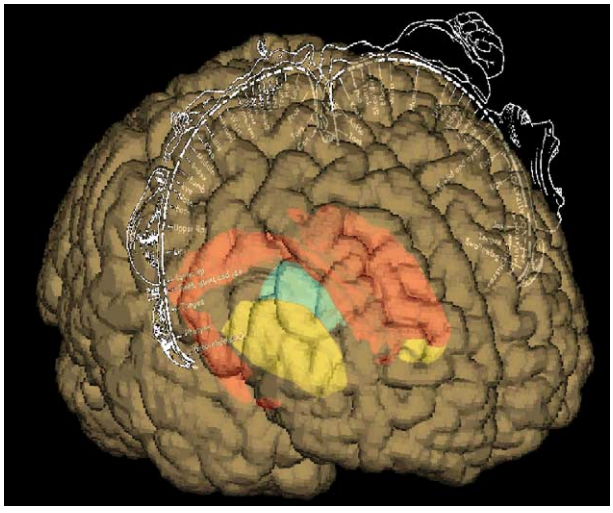

Fig. 6. Transparent display of a segmented cortex among with several 3D atlas structures (red: ventricles; cyan: thalamus; yellow: putamen) and with the homunculi of Penfield and Rasmussen (1950). The motoric homunculus is displayed in the left hemisphere, the somatosensoric in the right. (This figure is available in colour, see the on-line version.)

In our atlas system we implemented an interface to the Talairach Daemon, a neuroanatomic database developed by Lancaster et al. (2000), which is accessible through the Internet. [2] One can send the Talairach coordinates of a point of interest to this database, whereupon the database responds with informations concerning the point: A hierarchy of structures located in the vicinity of the point can be queried as well as the probabilities for the point being located in a certain structure. Accessing the Daemon from within our system is possible by simply clicking a location with the mouse; the information received from the database is then listed in a window along with the corresponding Talairach cooordinates. Table 2 lists some results acquired with the Daemon interface.

Furthermore, we have developed a database with additional textual and pictorial contents which can be accessed from within the atlas system by picking the atlas structures in the scene with the mouse. So far we have included the "Glossary of Structures and Definitions" from the "Atlas of Brain Function" by Orrison (1995), the glossaries contained in the atlases of Talairach and Tournoux (1988, 1993), and the textual description of the Brodmann areae according to Garay (1999), who translated the famous monograph of Brodmann (1909) to the English language. We formatted the descriptions in HTML and linked all terms hypertextually. To be sure to use an internationally accepted terminology, we present all names as proposed by the "Terminologia Anatomica" (FCAT, 1998). So far, our database contains more than 450 entries.

4.2. Accuracy

A question which is crucial for a computerized atlas system is its accuracy. We divide the accuracy considerations into two parts: (i) the precision of the digital

[2] http://ric.uthscsa.edu/projects/talairachdaemon.html.

Table 2
Some responses of the Talairach daemon database on queries concerning structures located at certain coordinates (upper part of the table) and concerning probabilities (lower part)

Coordinates			Hemisphere	Lobe	Gyrus	Tissue	Cell
−9	9	7	Left cerebrum	Sub-lobar	Caudate	Grey matter	Caudate body
−9	63	5	Left cerebrum	Frontal lobe	Medial frontal gyrus	White matter	*
46	−58	−27	Right cerebrum	Temporal lobe	Superior temporal gyrus	Grey matter	Brodmann area 39
3	−28	0	Right brainstem	Midbrain	*	*	*
			Structure	Probability			
−13	−14	18	Thalamus	52.94			
−16	−13	4	Thalamus	100.00			
−29	−54	13	Parietal lobe	1.96			
−14	17	13	Caudate	85.10			

The coordinates are distances to the commissura anterior given in mm (medio-lateral, antero-posterior, cranio-caudal, positive axes pointing to the right/front/top), the probabilities are given in %.

representation of the original printed material, and (ii) the quality of the mapping between atlas and patient.

4.2.1. Accuracy of the 3D atlas model

We studied the accuracy of our 3D reconstruction algorithm by cross-sectioning the surface models with the original atlas plates. As can be seen in Fig. 7, the contours match very well on the structures drawn in the plates. For this reason, we consider the digital representation as sufficient. Note, that partial inconsistencies between orthogonal plates, which are limits of the Talairach atlas, are still maintained in our digital plates, because we did not alter the scanned brain maps. The 3D reconstructed brain structures do not fit perfectly to the sagittal and axial plates at these inconsistent locations for the same reason. However, compared to the printed atlas book it is an advantage that the ambiguities become immediately obvious in the digital version.

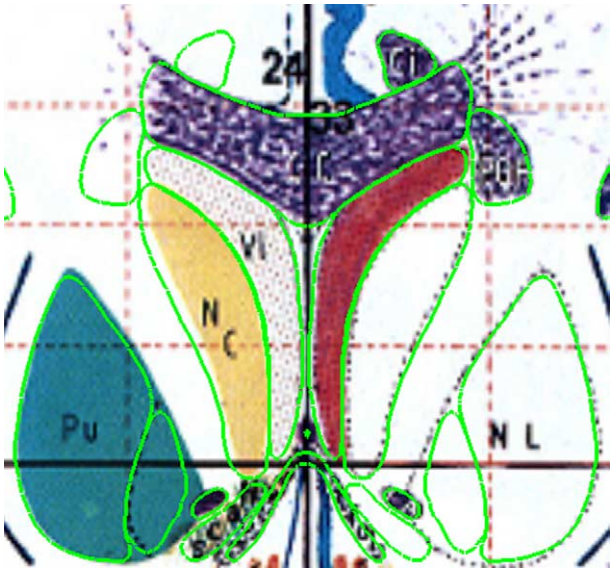

Fig. 7. Contours of several reconstructed objects (green) are drawn on a coronal plate taken from the Talairach and Tournoux (1988) atlas. The consistency is mostly well. The deviation at the nucleus caudatus (NC, yellow) in the right hemisphere is due to an asymmetry in Talairach's drawing: in the left hemisphere, the contour is placed correctly. (This figure is available in colour, see the on-line version.)

4.2.2. Accuracy of the nonrigid matching

We performed two examinations in order to assess quantitative measures for the matching accuracy. The first utilizes fMRI scans with activations on the precentral gyrus, and for the second we evaluated the position of the frontal tip of the putamen. For an interpretation of the results see Section 5.

The fMRI method: For our examination we used MRI datasets from 10 patients, into which functional activations of the primary motor cortex achieved by finger tapping have been inserted from a corresponding fMRI scan. Due to the activations, the precentral gyrus, on which the primary motor cortex is located, is easily identifiable in the MR images. We matched our atlas system nonrigidly to these datasets and analyzed the conformity between the corresponding precentral gyri in the atlas and the MR images. For the evaluation we superimposed matched axial atlas plates of the Talairach atlas on axial cross-sections of the MR datasets. In seven atlas plates (1_2, 2, 2_3, 3, 3_4, 4, 4_5) we measured the antero-posterior distance between the dorsal edges of the gyrus praecentralis in the atlas and in the MRI at up to six well-defined positions. Fig. 8 illustrates this procedure. Because the atlas plates are not parallel to the MR image due to the nonrigid deformation, we selected for each single measurement the axial MR cross-section having the smallest distance to the atlas plate at the measurement location. The measured distances are signed depending on which modality was more frontal. For determining the distances we used the interactive measuring tool of our atlas system. We performed these measurements for piecewise linear matching as well as for nonrigid matching using the $\psi_{3,0}$ basis function and

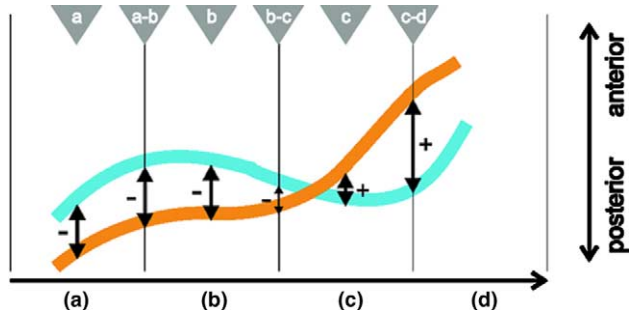

Fig. 8. Schematic drawing of a axial slice, in which the borders of the corresponding motor cortices of the atlas (orange) and of an MR image (blue) are shown. The characters *a* to *d* correspond to the lateral coordinates of the proportional grid of Talairach's atlas. Antero-posterior distances at six positions (indicated by the grey triangles and the double-headed arrows) are evaluated if the gyrus praecentralis was determinable in the MR image at the accordant lateral position. (This figure is available in colour, see the on-line version.)

the Thin Plate Spline basis function in order to assess the influence of different matching parameters. Table 3 contains the acquired measurements, listed separately for each of the considered atlas plates.

The Putamen method: For this examination we used MRI datasets from 24 patients, in which the frontal tip of the putamen was identifiable. We again matched our atlas system nonrigidly to these datasets and measured the distance of this tip between atlas and MR image. Table 4 contains the acquired measurements.

4.3. Applications

In the following, we illustrate the applicability of our atlas system with some practical examples. The first deals with a patient having a large tumor in the right hemisphere, which causes a noticeable shift of the midsagittal plane towards the left hemisphere. We matched our atlas to this individual in four different ways: linearly (i.e. adaption of the brain size), piecewise linearly (i.e. adaption according to Talairach's proportional grid), nonrigidly without considering the tumor, and nonrigidly with taking the tumor into account. In Fig. 9 the results of all four approaches can be compared. Obviously, the nonrigid approach regarding the tumor performs best. As an additional illustration of the best matching result, Fig. 10 shows some further cross-sections through the brain as well as a 3D scene of this case.

Table 4
Results of the evaluation of distances at the frontal tip of the putamen between the atlas and MR datasets ($N = 24$) for three different matching approaches

Matching	Hemisphere	
	Left	Right
	$\bar{d} \pm$ SD	$\bar{d} \pm$ SD
Grid	5.15 ± 2.40	4.83 ± 2.39
Thin Plate Spline	5.62 ± 1.93	5.89 ± 2.90
$\psi_{3,0}$	4.76 ± 2.03	3.99 ± 1.76

The mean and standard deviation values are given in mm. For further explanations see the text.

In the second case we matched the atlas nonrigidly to a MR scan acquired during surgery with an open MR scanner (Magnetom Open, Siemens, Erlangen, Germany). As can be seen in Fig. 11, the brain underwent a tumor resection and is affected by a noticeable amount of brain shift. Fig. 12 shows the segmented cortex of this case in which likewise the resection cavity is clearly visible. Furthermore, the point correspondences at the cortex which were established for the nonrigid matching are displayed in this scene. Of course the longest displacement vectors occur in the brain-shifted region. The neurosurgeon now can lay informations from the adapted atlas over the MR images, which can support his decision whether to proceed with resection or not. Especially in images of poor quality, like intraoperative ones, additional informations are highly welcome. Fig. 11 clearly shows that the atlas adapted very well to the shape of the deformed brain. Fig. 13 grants a 3D impression of the deformations which happened in this case. Though we performed the matching procedure retrospectively after the intervention, we could have done it during surgery as well, because the total amount of time needed for interaction and processing was just about 25 min. Matching the atlas to intraoperative scans has a useful side effect, too. Because patients normally

Table 3
Results of the evaluation of distances at the gyrus praecentralis between the atlas and MR datasets ($N = 10$) for three different matching approaches

Matching		Atlas plate							
		1_2	2	2_3	3	3_4	4	4_5	Total
Grid	$\bar{d}$	−3.54	−4.36	−1.55	−2.03	−1.87	−0.83	−1.07	−2.37
	d_{RMS}	6.24	6.44	4.92	6.09	4.75	5.48	5.42	5.68
Thin Plate Spline	$\bar{d}$	−0.86	−1.36	−0.47	−0.88	1.29	1.95	3.52	0.07
	d_{RMS}	5.23	4.77	3.79	3.51	4.18	4.87	5.15	4.46
$\psi_{3,0}$	$\bar{d}$	0.14	−0.89	0.38	0.11	1.53	1.39	2.58	0.50
	d_{RMS}	4.38	4.58	4.12	3.03	4.22	3.07	3.85	3.96

The mean and root mean square (RMS) values are given in mm. For further explanations see the text.

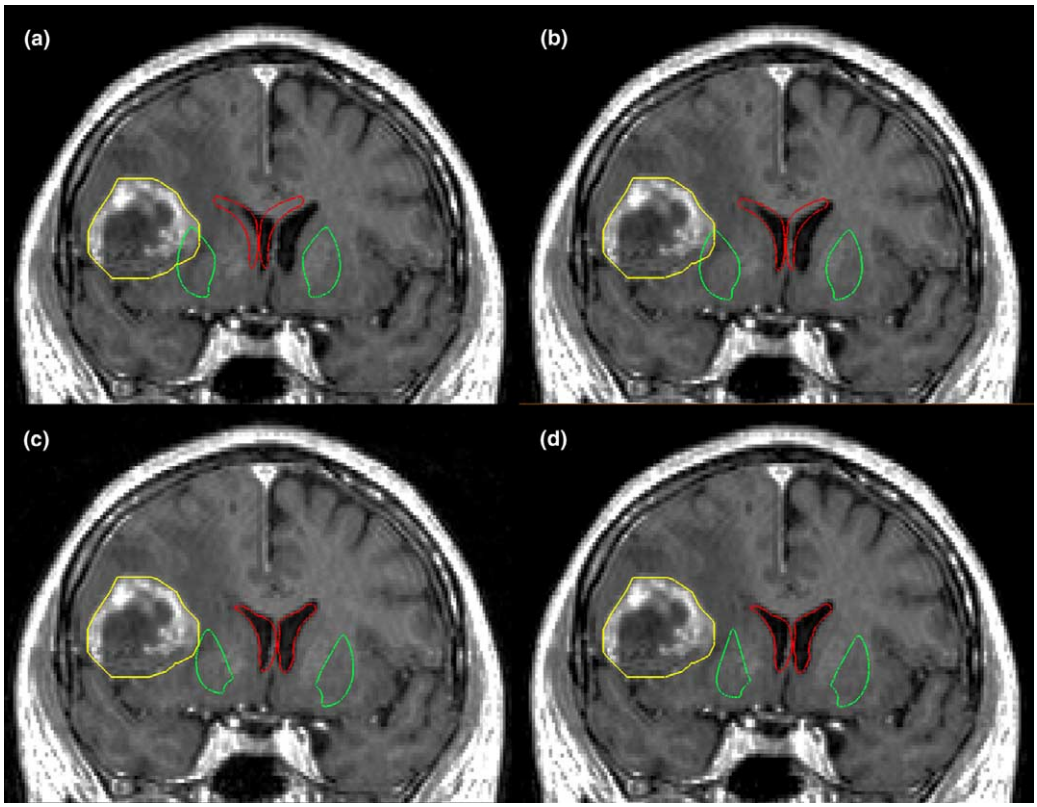

Fig. 9. Comparison of four matching paradigms: (a) linear; (b) piecewise linear; (c) nonrigid without tumor; (d) nonrigid with tumor. In a coronal MR cross-section the contours of the lateral ventricles (red) and the putamen (green) are displayed in relation to the contour of the segmented tumor (yellow). While in the first two cases the right putamen intersects the tumor and the ventricles do not match very well, the nonrigid approaches yield good results. Especially the ventricles and the left putamen are positioned excellently. While it is not very likely that the right putamen touches the tumor (as in case c), the additional forces inside the tumor, which shift the putamen further to the midline, are obviously necessary. (This figure is available in colour, see the on-line version.)

do not lie on their back during surgery, intraoperative images frequently depict the patient's head in very strange positions, which makes orientation difficult. During the grid matching step, the MR dataset gets resliced parallel to the CA–CP plane, the standard imaging plane; this way, orientation gets much easier.

A third case illustrates the application of our atlas for a stereotactic intervention. Two electrodes have been inserted in the patient's thalamus for electrical deep brain stimulation (a two-sided stimulation of the ventro-intermediate nucleus VIM, which is part of the ventro-lateral nucleus VL); their trajectories are visible as hypointense spots in the MR scans, and they have been tagged in the atlas system using the drawing tool. By visualizing the thalamic nuclei as well, the physician is able to check the location of the tip of his probes against the atlas. In the case example the right electrode's tip actually is inserted in VL, while the left one is between VL and NA. The situation is depicted in Fig. 14. As in the previous case, the atlas was applied retrospectively to the images. The atlas system is not suited to perform targeting in stereotactic interventions, but it allows for an additional visual control during the intervention.

5. Discussion

5.1. Three-dimensional reconstruction

The 3D reconstruction algorithm yields accurate and smooth surface models of most of the brain structures contained in the atlas book. However, it is not suited for reconstructing cortex and Brodmann areae, which therefore are not represented three-dimensionally in our atlas system. This is mainly due to the wide gaps between the Talairach plates: there is too much information missing about the complex shape of the cortical convolutions, which can not be compensated by simple interpolation.

As opposed to the atlas of the Singapore group, who does not interpolate additional slices during their 3D reconstruction, our discrete volume dataset is more isotropic, and therefore our spatial smoothing filter needs not to be as strong. In addition, because we only process one hemisphere, the problem of elimination of small gaps along the midsagittal plane like the septum pellucidum, which separates the lateral ventricles, can not appear in our approach. Fang et al. (1995) address this problem by defining a location-dependent smooth-

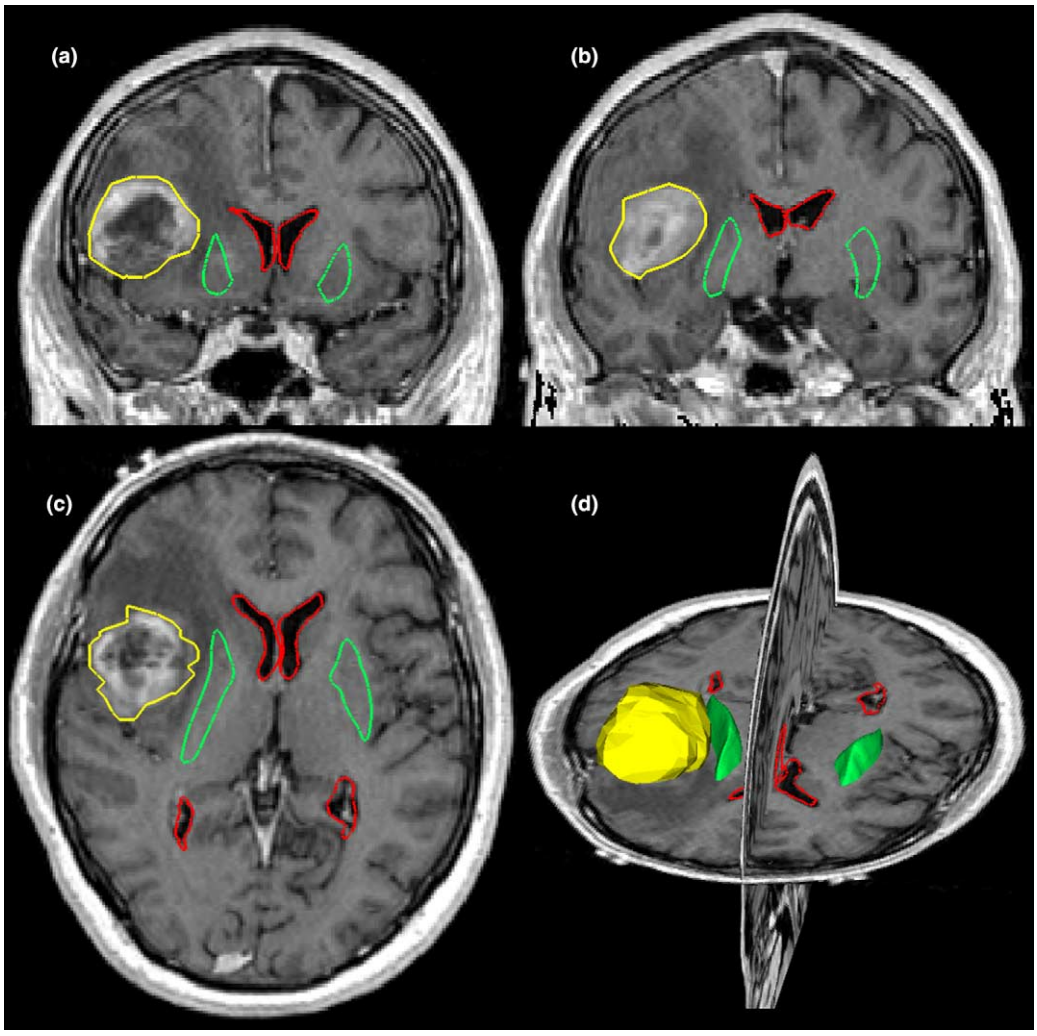

Fig. 10. Some images which further illustrate the best matching result from Fig. 9(d). The two coronal cross-sections show cuts through the brain located more frontal (a) respectively more occipital (b) than in Fig. 9. In (c) an axial cross-section is displayed, and (d) shows a 3D view. The lateral ventricles are again shown in red, the putamen in green and the segmented tumor in yellow. It can clearly be seen that the tumor pushed the right putamen towards the left hemisphere. (This figure is available in colour, see the on-line version.)

ing which conserves these structures at the price of less smooth objects near the midline.

In principle, our interpolation approach is suitable for generating an arbitrary number of slices between two given ones. Two reasons are responsible for our choice to generate only one. The first is that we use the marching cubes algorithm for surface extraction, which is well known to produce an overwhelming amount of very small triangles. If we had produced an even bigger binary volume, the number of resulting triangles would have exploded, while their area would have become smaller and smaller. A decimation step necessary to be able to visualize and process these models would have largely eliminated the benefit from the finer granularity. The second reason is, that with the Nuages algorithm we achieve a linear interpolation between the shapes. We assume that, apart from only a few locations, we would not have seen noticeable effects from interpolating more than one slice. There is an approach known from the literature which is capable of smoothing triangular surface meshes (Leventon and Gibson, 1999). It would be interesting to try whether our reconstructed atlas structures could be further improved using this algorithm.

5.2. Segmentation

Though the segmentation approach we use is relatively simple, it has proved to work well even for images of comparatively bad quality, like intraoperative scans. For visualization as well as for providing target structures the demands on the accuracy of the segmentation results are not too high. This is reasonable for the visualization case. In case of the target structures, one has to keep in mind that they are used to establish displacement vectors, i.e. they get sampled, which reduces

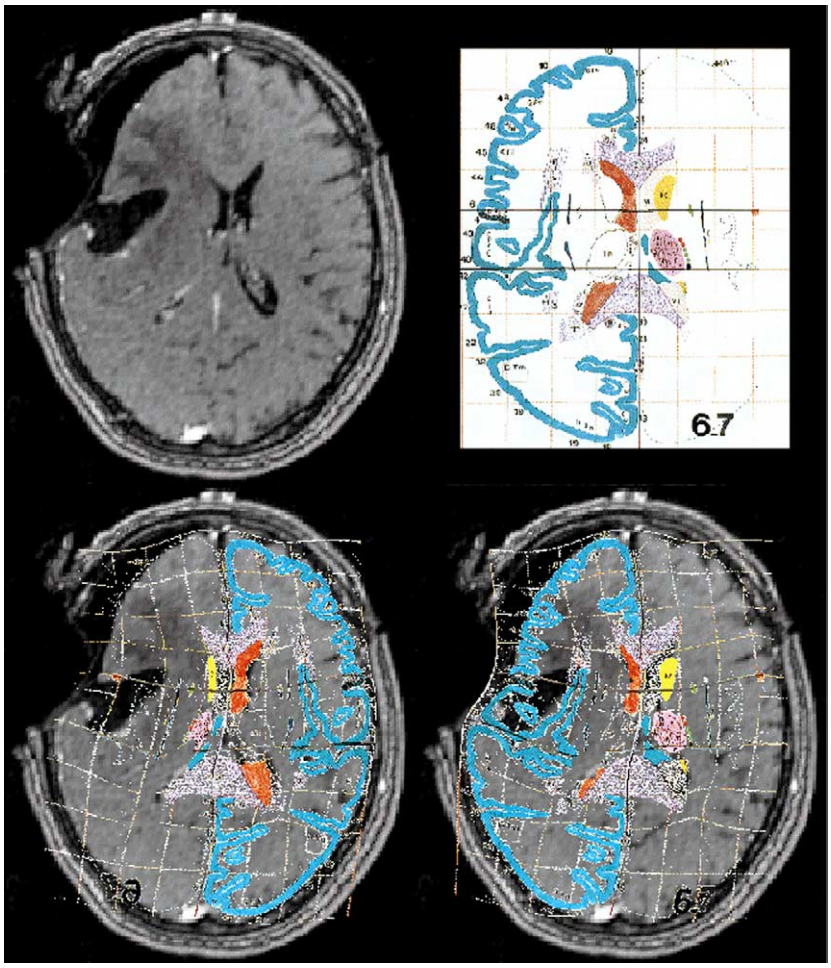

Fig. 11. The atlas was matched nonrigidly to a MRI dataset acquired during surgery. The atlas compensates the large deformation (brain shift) caused by the intervention. Top row: axial image (left), original axial plate from the atlas of Talairach and Tournoux (1988) (right). Bottom row: transparent overlay of the nonrigidly deformed plate on both hemispheres. In the insula as well as at the left ventricle the matching seems to be inaccurate. This can be explained as follows: (i) the insula is relatively far apart from the given point correspondences, so the amount of uncertainty is relatively big; (ii) the axial atlas plate is deformed not only in-plane, but also perpendicular to the plane (a similar effect can be seen for coronal and sagittal plates in Fig. 13). The image of course depicts a projection of the deformed plate onto a plane MR cross-section, while the actual distance between MR image and deformed plate at some locations is up to several millimeters. (This figure is available in colour, see the on-line version.)

their overall shape to several hundreds of surface points (the cortex segment additionally is transformed to its envelope). So it is clear that not each single voxel matters.

As mentioned above, segmentation lasts only a few minutes, and user interaction is limited to choosing appropriate operations. Nevertheless it would be nice to have a fully automated algorithm, in the best case one that would be able to segment tumors as well. Several automatic brain segmentation approaches have been published (Aboutanos et al., 1999; Smith, 2002). However we are not aware of an approach being adaptable to our application without major changes. For example, the algorithm of Smith (2002) is not able to segment the ventricles as it is needed for our application, and that of Aboutanos et al. (1999) is much too slow (it takes more than one hour to segment a brain volume). By the way, it is our experience that physicians like to have the possibility of taking influence on the result at each step of the segmentation, especially when images containing pathologic situations have to be processed.

5.3. Piecewise linear matching

Our approach for piecewise linear matching, which requires interactive adjustment of the proportional grid, works fast, and its handling is accepted by the physicians. However, several groups have developed algorithms for establishing the proportional grid fully automatically. Kruggel and von Cramon (1999) did this for MR images, Minoshima et al. (1993) for PET images. Because these approaches are described to be very robust, we plan to implement an automatic method like that of Kruggel and von Cramon (1999) in our system.

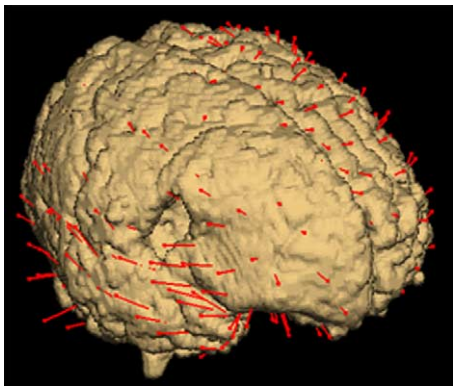

Fig. 12. Three-dimensional visualization of a cortex in an intraoperative MR scan (same patient as in Fig. 11) along with the cortex displacement vectors (red) established for the nonrigid matching. Of course the longest displacement vectors are in the region where brain shift is most dominant (caudal to the resection cavity). (This figure is available in colour, see the on-line version.)

5.4. Nonrigid matching

As mentioned, several working groups within the medical domain have used radial basis functions in the context of nonrigid matching. The approach is well suited for interpolation purposes, but has the disadvantage of not being able to account for mechanical properties of underlying structures. Applications like e.g. calculating a forecast of brain shift would need this ability. For our application however this is not a problem, because matching of two distinct brain instances is more a mathematical than a physical procedure.

An advantage of radial basis functions is that they lead to linear equation systems. Numerous algorithms are known to solve these. Physically motivated approaches like finite element models likewise lead to linear equation systems, which however are usually much bigger. In addition, the finite element method requires a discretization of the continuum, which has to be achieved by means of meshing.

5.5. Determination of point correspondences

Establishing point correspondences is an important step for the matching procedure, because the displacement vectors determine the maximal accuracy. Though as much point correspondences as possible should be used, and though they ideally should be spread equally throughout the whole volume, they can of course only be established at locations where brain structures can be clearly identified in the MR images. Unfortunately, there is a relatively wide gap between cortex and ventricles where no structures are visible with sufficient contrast. One potential candidate in the mentioned gap is the putamen, but its contrast in MR images is rather low, for which reason an automatic placement of landmarks on it is very difficult. Because the given displacement vectors will be interpolated by the radial basis functions, it is not a solution to simply establish more point correspondences at the structures already in use (cortex and ventricles). Due to the distance, for a point located e.g. in the putamen it does not make any difference if we interpolate 200, 2000 or 20000 vectors at the cortex level.

Thompson and Toga (1996) proposed a surface-based technique for matching 3D images of the brain, in which several similar ideas are treated. First of all, they likewise look for corresponding points at the cortex, at sulci and at the ventricles, and they interpolate these correspondences to the whole brain as well. Furthermore, they also assume cortex points to lay on the cortex's envelope and perform a redistribution of cortex points such that sulcus correspondences are taken into account. One major difference is that they represent sulci as 2D ribbons running between the two adjacent gyri, rather than just as lines as we do. The ribbon representation has the advantage that correspondences are established not only at the brain surface, but also in the bottoms of the sulci which obviously lay deeper in the brain. The user has to interactively tag the sulci in the work of Thompson and Toga as well; it is clear that tagging a ribbon is much more labour intensive than tagging a line. Correspondences between the ribbons are established by mapping the ribbons to the unit square and linking locations having the same unit square coordinates. Obviously, our approach for finding corresponding points on sulcus lines is the one-dimensional (1D) equivalent to that.

A somewhat different approach for establishing correspondences on the brain surface is proposed by Warfield et al. (2002) and Ferrant et al. (2002). For their finite element based 3D brain warping approach they use an active surface algorithm which iteratively deforms surfaces of both brain and ventricles from the source image to match that of the target image. The forces for the active surface, which behaves like an elastic membrane, are derived from image intensity gradients. The constraints for the 3D warping are point correspondences on these surfaces which define given displacement vectors in the FE model. While this approach results in a good congruency of the overall shapes, it seems not to guarantee that corresponding anatomical features like certain gyri or sulci actually result in corresponding points.

In cases where tumors deform central brain regions, the piecewise linear matching does not necessarily lead to coincidence of commissures in atlas and patient. To be able to deal with such cases, our system forces the user to confirm for both the anterior and the posterior commissure whether fixpoints should be added.

Our approach for modelling tumor growth surely is a simplification of reality. We believe that the assumption

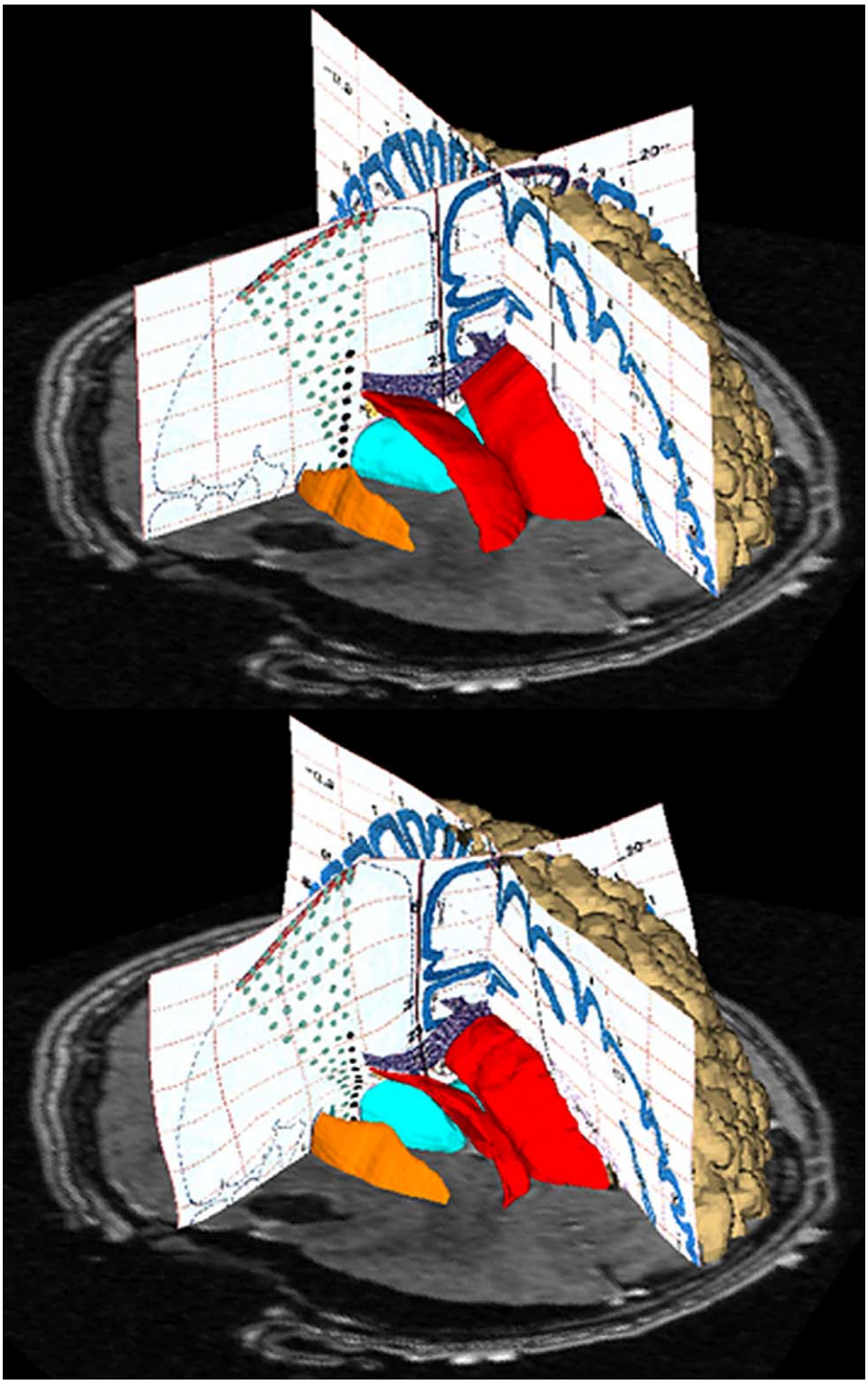

Fig. 13. A 3D scene showing several items from the atlas along with an axial MR cross-section and the left hemisphere of the segmented cortex of an intraoperative MR scan (same patient as in Figs. 11 and 12). Top: piecewise linear matching; bottom: nonrigid matching. It is clearly visible, that the atlas structures (red: ventricles; cyan: thalamus; orange: claustrum) did move along with the direction of the brain shift. (Atlas plates are taken from the atlas of Talairach and Tournoux, 1988.) (This figure is available in colour, see the on-line version.)

of radially directed growth (isotropy) only in rare cases exactly holds. Nevertheless, it seems to be a reasonal assumption: Kansal et al. (2000) studied and simulated brain tumor growth successfully using an isotropic model, and Kyriacou et al. (1999) relied on it in their work as well. It is obvious that with our approach it

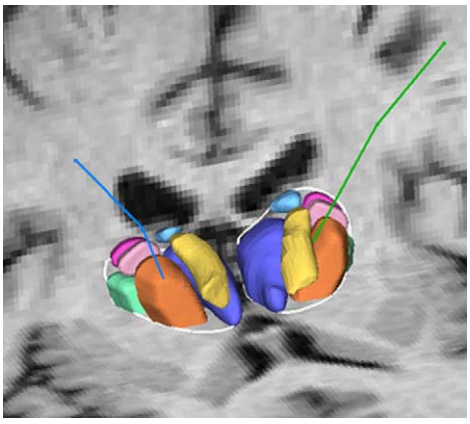

Fig. 14. A physician inducted two electrodes (green, blue) in a patient's brain during a stereotactic intervention (deep brain stimulation). The atlas was nonrigidly matched to the brain, and after displaying the thalamic nuclei (coloured structures), the position of the probes' tips can be judged. The contour of the thalamus is drawn as white line on the MR scans. (This figure is available in colour, see the on-line version.)

would be possible to model non-isotropic tumor growth as well by defining appropriate displacement vectors. So far, we did try to compensate only deformations due to tumors, but we believe that our approach could be adapted to some other deforming brain pathologies as well, e.g. to strokes, as long as they can be segmented.

5.6. Neuronavigation support

Any tool assisting surgical planning can develop its full potential only if the planning information can be transferred to the patient during surgery. This is the reason why we implemented an interface to a neuronavigation system. Compared with other fields of medical image processing, the literature concerning anatomic atlases in the context of navigation systems is rather sparse. While there are a few publications dealing with proprietary brain atlases (e.g. Niemann et al., 1999, Levy et al., 1997), to our knowledge the only other Talairach atlas system which can cooperate with navigation hardware is that of the Singapore group. So navigation support is one further aspect which dissociates our system against most Talairach based atlas systems.

5.7. Inclusion of further information

We intended to offer to the user as much neurological information as possible without additional effort, i.e. without the need to perform additional matching steps. For this reason we included additional visual items carrying complementary information, as well as textual information verbally describing structures or providing statistical material concerning brain anatomy.

An oftenly mentioned limitation of the Talairach atlas is, that it depicts only a single brain. The interface to the Talairach Daemon which we implemented in our system partially overcomes this disadvantage, because the Talairach Daemon provides probabilistic information on brain structures. Though the main intention of the Talairach Daemon is in the field of brain mapping, neurosurgical planning can profit from it, too. Imagine e.g. a surgeon being interested in the probability of a certain coordinate, which might lay on a potential trajectory, to be located in some important brain structure.

A further problem is the absence of the cerebellum in the Talairach atlas. We did not account for this so far, for which reason our atlas system is limited to the cerebrum. To address this, we plan to include a cerebellum atlas like the one recently published by Schmahmann et al. (2000). Fortunately, this monograph utilizes a caudal extension of the proportional grid to present the data; it should be not too hard to make this atlas available in our system.

An other aspect makes the inclusion of further information desirable, too. Besides of the usage in the neurosurgical context, the atlas system is well suited for serving as a teaching system for neuroanatomy. The intuitive presentation of the anatomical knowledge makes it easy to comprehend interrelations between the involved structures, and the state-of-the-art technology (3D visualization with real-time interaction and response, hypertext documents) clearly outperforms a printed book containing comparable information. The use of HTML-formatted texts allows the inclusion of further media in the system, e.g. pictures, videos and sounds.

Being faced with the limitations of the Talairach atlas, one could argue that it would be better to use a totally different brain atlas for building the atlas system. Our segmentation method is independent of the atlas anatomy, so this step is not crucial. However, the matching procedure forces an atlas to meet two constraints: It must make use of the proportional grid as coordinate system (for the piecewise linear pre-registration), and it must depict the cortex, which is used as target structure in the nonrigid matching. The "Atlas of the Human Brain" by Mai et al. (1997) e.g. fulfills both constraints, whereas the atlas by Schaltenbrand and Wahren (1977) neither uses the grid nor shows the cortex.

5.8. Accuracy

(a) *The fMRI method*: It is obvious that the nonrigid matching approaches perform better than the grid matching; the $\psi_{3,0}$ matching is the best in our examination, because the mean as well as RMS values of the distances are smallest for this basis function. Because our distance values are signed, we theoretically expect mean values around 0 (this would indicate that no systematic error is present). While this is approximately true for the nonrigid methods, the grid matching

obviously is affected by a systematic shift (i.e. the location of the precentral gyrus in the atlas seems to be systematically different in relation to the commissures than in the other brains we considered). This shift is corrected by the nonrigid matching. The RMS values allow for an estimate of the error which we have to expect. It can be seen that this error is nearly independent from the position in the brain (here: on each atlas plate), and that for the best approach ($\psi_{3,0}$) it amounts to 4 mm. It should however be kept in mind that measuring the distances strictly in antero-posterior direction is a rather conservative method (imagine the case where both gyri are running parallel with small distance in nearly antero-posterior direction!).

(b) *The putamen method*: It is obvious that the Thin Plate Spline (TPS) matching performs worse than the grid matching. This probably is due to the non-locality of the TPS basis functions. The nonrigid $\psi_{3,0}$ matching performs slightly better than the grid matching. However, the distances remain relatively large ($\geqslant 4$ mm). Two reasons might be responsible for this: (i) The tip of the putamen has been identified incorrectly in the MR datasets (note that the putamen is not always sharply demarcated in the scans, and that at the resolution of the MR scan ($1 \times 1 \times 1.3$ mm^3) a mislocation of just one voxel in each direction leads to a distance of $\sqrt{(1^2 + 1^2 + 1.3^2)}$ mm$^2 = 1.9$ mm), and (ii) the nonrigid matching can not improve the accuracy significantly at locations being remote to its constraints. The reason why TPS performed better than the grid in the fMRI method, but worse than the grid in the putamen method is that in the fMRI method the constraints (given point correspondences) are located nearer to the points of measurement than in the putamen method.

The main goal for the nonrigid matching is to improve the piecewise linear matching which is provided by the proportional grid. As the evaluations show, this goal is fulfilled by the nonrigid $\psi_{3,0}$ matching approach. Further evaluations should be conducted in order to increase the number of cases (neither $N = 10$ as in the fMRI method, nor $N = 24$ as in the putamen method can provide statistically sound results).

5.9. Implementation of an atlas system

We chose the Win32 platform for our atlas system because it guarantees wide acceptance by physicians, who are used to it. Because most of today's consumer graphics boards provide hardware OpenGL acceleration (in order to step up gaming performance), the system runs very fast on typical PC hardware. A 500 MHz CPU and 256 MB of memory are sufficient for running the application. These very moderate demands make the system attractive for clinical environments.

For numerically solving the linear equation systems of the nonrigid matching, we use the *Portable Extensible Toolkit for Scientific Computation* (*PETSc*) from the Argonne National Laboratories (Balay et al., 2000), which is distributed freely via the Internet. [3]

6. Summary

We have developed a computerized atlas system based on the Talairach atlas which fulfills the requirements stated in the beginning of this paper (see Section 1). Therefore it not only overcomes principal drawbacks of printed anatomic atlas books, but also the limitations of the Talairach atlas itself: The 3D representation of atlas structures overcomes the two-dimensionality and sparseness of the atlas book, Talairach's assumption of left/right symmetry of the brain is addressed by the nonrigid matching capability, and the possibility to simultaneously display original atlas plates of different orientation in the 3D scene defuses the problem of inconsistent plates, because the ambiguities become obvious to the user (nevertheless there is a small amount of inaccuracy due to these; we however believe that with some diligence these inconsistencies could be eliminated in the original atlas data).

The easy-to-handle matching capability in conjunction with the visualization features allows for convenient transfer of atlas information to individual patient datasets with satisfying accuracy. Especially the nonrigid registration with its capability to consider tumors is a novel and valuable property. The interface to a navigation system is a need-to-have prerequisite indispensable for the intraoperative application. To our knowledge, our system is the first to have *all* of the following features: presenting well-established anatomical contents from different sources, being 3D, including very fast segmentation tools, including an interface to a navigation system, offering a nonrigid matching capability, and being able to handle anatomies potentially being deformed due to tumors. Furthermore, because the temporal performance of our system is very good, it is well suited for usage in the time-critical clinical environment. The only other system which also offers nonrigid matching of a 3D Talairach atlas (Xu and Nowinski, 2001) is one order of magnitude slower than ours.

Acknowledgements

We would like to thank the reviewers for their valuable comments on the manuscript.

[3] http://www-fp.mcs.anl.gov/petsc/

References

Aboutanos, G.B., Nikanne, J., Watkins, N., Dawant, B.M., 1999. Model creation and deformation for the automatic segmentation of the brain in MR images. IEEE Trans. Biomed. Eng. 46 (11), 1346–1356.

Arad, N., Reisfeld, D., 1995. Image warping using few anchor points and radial functions. Comput. Graph. Forum 14 (1), 35–46.

Balay, S., Gropp, W.D., McInnes, L.C., Smith, B.F., 2000. PETSc Users Manual. Tech. Rep. ANL-95/11 – Revision 2.1.0, Argonne National Laboratory.

Barillot, C., Lemoine, D., Gibaud, B., Toulemont, P.J., Scarabin, J.M., 1990. A PC software package to confront multimodality images and a stereotactic atlas in neurosurgery. SPIE Med. Imaging IV: Image Capture and Display 1232, 188–199.

Borgefors, G., 1984. Distance transformations in arbitrary dimensions. Computer Vision Graph. Image Process. (27), 321–345.

Brodmann, K., 1909. Vergleichende Lokalisationslehre der Großhirnrinde. Verlag von Johann Ambrosius Barth, Leipzig.

Chunguang, J., Ou, T., Huilong, D., Weixue, L., 1998. Multimodality brain atlas on the visible Human Project Dataset. In: Conference Proceedings IEEE Engineering in Medicine and Biology, 20th Annual International Conference, pp. 556–558.

Davatzikos, C., 1996. Spatial normalization of 3D brain images using deformable models. J. Comput. Assist. Tomogr. 20 (4), 656–665.

Davatzikos, C., Prince, J.L., Bryan, R.N., 1996. Image registration based on boundary mapping. IEEE Trans. Med. Imaging 15 (1), 112–115.

Dickhaus, H., Eisenmann, U., Ganser, K.A., Metzner, R., Wirtz, C.R., 2002. A multimodal computer based system for neurosurgical interventions. In: Proceedings of the 12. Nordic Baltic Conference on Biomedical Engineering and Medical Physics NBC, June 2002.

Evans, A.C., Kamber, M., Collins, D.L., MacDonald, D., 1994. An MRI-based probabilistic atlas of neuroanatomy. In: Shorvon, S.D. (Ed.), Magnetic Resonance Scanning and Epilepsy. Plenum Press, New York, Chapter 48, pp. 263–274.

Fang, A., Nowinski, W.L., Nguyen, B.T., Bryan, R.N., 1995. Three-dimensional Talairach–Tournoux brain atlas. SPIE Med. Imaging 1995: Image Display 2431, 583–592.

Federative Committee on Anatomical Terminology (FCAT), 1998. Terminologia Anatomica. Georg Thieme Verlag, Stuttgart, New York.

Ferrant, M., Nabavi, A., Macq, B., Black, P.M., Jolesz, F.A., Kikinis, R., Warfield, S.K., 2002. Serial registration of intraoperative MR images of the brain. Med. Image Anal. 6 (4), 337–359.

Fornefett, M., Rohr, K., Stiehl, H.S., 2001. Radial basis functions with compact support for elastic registration of medical images. Image Vision Comput. 19, 87–96.

Garay, L., 1999. Brodmann's Localisation in the Cerebral Cortex. Imperial College Press, London.

Garlatti, S., Sharples, M., 1998. The use of a computerized brain atlas to support knowledge-based training in radiology. Artif. Intelligence Med. 13, 181–205.

Geiger, B., 1993. Three-dimensional modeling of human organs and its application to diagnosis and surgical planning. Tech. Rep. RR No. 2105, Institut National de Recherche en Informatique et en Automatique INRIA.

Höhne, K.-H., Hanson, W.A., 1992. Interactive 3D segmentation of MRI and CT volumes using morphological operations. J. Comput. Assist. Tomogr. 16 (2), 285–294.

Kansal, A.R., Torquato, S., Harsh, G.R., Chiocca, E.A., Deisboeck, T.S., 2000. Simulated brain tumor growth dynamics using a three-dimensional cellular automaton. J. Theor. Biol. 203, 367–382.

Kelly, P.J., 1996. Computer-assisted neurosurgery: needs and opportunities. In: Taylor, R.H., Lavallée, S., Burdea, G., Mösges, R. (Eds.), Computer Integrated Surgery – Technology and Clinical Applications. The MIT Press, Cambridge, MA, pp. 301–306.

Kruggel, F., von Cramon, Y., 1999. Alignment of magnetic-resonance brain datasets with the stereotactical coordinate system. Med. Image Anal. 3 (2), 175–185.

Kyriacou, S.K., Davatzikos, C., Zinreich, S.J., Bryan, R.N., 1999. Nonlinear elastic registration of brain images with tumor pathology using a biomechanical model. IEEE Trans. Med. Imaging 18 (7), 580–592.

Lancaster, J.L., Fox, P.T., 2000. Talairach space as a tool for intersubject standardization in the brain. In: Bankman, I.N. (Ed.), Handbook of Medical Imaging – Processing and Analysis, first ed. Academic Press, New York, Chapter 35, pp. 555–567.

Lancaster, J.L., Woldorff, M.G., Parsons, L.M., Liotti, M., Freitas, C.S., Rainey, L., Kochunov, P.V., Nickerson, D.S., Mikiten, S., Fox, P.T., 2000. Automated Talairach atlas labels for functional brain mapping. Hum. Brain Mapp. 10, 120–131.

Lemoine, D., Barillot, C., Gibaud, B., Pasqualini, E., 1991. An anatomical-based 3D registration system of multimodality and atlas data in neurosurgery. In: Information Processing in Medical Imaging – Lecture Notes in Computer Science. Springer-Verlag, Berlin, pp. 154–164.

Leventon, M.E., Gibson, S.F.F., 1999. Generating models from multiple volumes using constrained elastic surface nets. Tech. Rep. Technical Report TR-99-09, Mitsubishi Electric Research Laboratory MERL.

Levy, A.V., Schaewe, T., Miller, M., Smith, K., Hammond, A., Henderson, J., Joshi, S., Mark, K.E., Sturm, C.D., McDurmont, L.L., Bucholz, R.D., 1997. An Internet-connected, patient-specified, deformable brain atlas integrated into a surgical navigation system. J. Digit. Imaging 10 (3), 231–237.

Lorensen, W.E., Cline, H.E., 1987. Marching cubes: a high resolution 3-D surface reconstruction algorithm. Comput. Graph. 21 (4), 163–169.

Mai, J.K., Assheuer, J., Paxinos, G., 1997. Atlas of the Human Brain. Academic Press, San Diego, London, Boston.

Mazziotta, J.C., Toga, A.W., Evans, A.C., Fox, P.T., Lancaster, J.L., Zilles, K., Woods, R.P., Paus, T., Simpson, G., Pike, B., Holmes, C., Collins, D.L., Thompson, P.M., MacDonald, D., Iacoboni, M., Schormann, T., Amunts, K., Palomero-Gallagher, N., Geyer, S., Parsons, L., Narr, K., Kabani, N., Goualher, G.L., Feidler, J., Smith, K., Boomsma, D., Pol, H.H., Cannon, T., Kawashima, R., Mazoyer, B., 2001. A four-dimensional probabilistic atlas of the human brain. J. Am. Med. Inform. Assoc. 8 (5), 401–430.

Melax, S., 1998. A simple, fast, and effective polygon reduction algorithm. Game Developers Mag. 11, 44–49.

Migneco, O., Darcourt, J., Benoliel, J., Martin, F., Robert, P., Bussiere-Lapalus, F., Mena, I., 1994. Computerized localization of brain structures in single photon emission computed tomography using a proportional anatomical stereotactic atlas. Comput. Med. Imaging Graph. 18 (6), 413–422.

Minoshima, S., Koeppe, R.A., Mintun, M.A., Berger, K.L., Taylor, S.F., Frey, K.A., Kuhl, D.E., 1993. Automated detection of the intercommissural line for stereotactic localization of functional brain images. J. Nucl. Med. 34, 322–329.

Nielsen, F.A., Hansen, L.K., 1998. Neuroinformatics based on VRML. Neuroimage 7 (4), S782.

Niemann, K., van den Boom, R., Haeselbarth, K., Afshar, F., 1999. A brainstem stereotactic atlas in a three-dimensional magnetic resonance imaging navigation system: first experiences with atlas-to-patient registration. J. Neurosurg. 90, 891–901.

Nowinski, W.L., Fang, A., Nguyen, B.T., Raphel, J.K., Jagannathan, L., Raghavan, R., Bryan, R.N., Miller, G.A., 1997. Multiple brain atlas database and atlas-based neuroimaging system. Comput. Aided Surg. 2, 42–66.

Orrison, W.W., 1995. Atlas of Brain Function. Georg Thieme Verlag, New York, Stuttgart.

Ou, T., Chunguang, J., Huilong, D., Weixue, L., 1998. Automatic segmentation and classification of human brain images based on TT atlas. In: 20th Annual International Conference IEEE Engineering in Medicine and Biology, 1998, pp. 700–702.

Penfield, W., Rasmussen, T., 1950. The Cerebral Cortex of Man. MacMillan Company, New York.

Schaltenbrand, G., Wahren, W., 1977. Atlas for Stereotaxy of the Human Brain. Georg Thieme Verlag, Stuttgart, New York.

Schiemann, T., Höhne, K.-H., Koch, C., Pommert, A., Riemer, M., Schubert, R., Tiede, U., 1994. Interpretation of tomographic images using automatic atlas lookup. SPIE Visualization Biomed. Comput. 2359, 457–465.

Schmahmann, J.D., Doyon, J., Toga, A.W., Petrides, M., Evans, A.C., 2000. MRI Atlas of the Human Cerebellum. Academic Press, San Diego, London, Boston.

Smith, S.M., 2002. Fast robust automated brain extraction. Hum. Brain Mapp. 17 (3), 143–155.

Talairach, J., Tournoux, P., 1988. Co-planar Stereotaxic Atlas of the Human Brain. Georg Thieme Verlag, Stuttgart.

Talairach, J., Tournoux, P., 1993. Referentially Oriented Cerebral MRI Anatomy. Georg Thieme Verlag, Stuttgart, New York.

Thompson, P.M., Toga, A.W., 1996. A surface-based technique for warping 3-dimensional images of the brain. IEEE Trans. Med. Imaging 15 (4), 1–16.

Thurfjell, L., Bohm, C., Bengtsson, E., 1995. CBA – an atlas-based software tool used to facilitate the interpretation of neuroimaging data. Comput. Meth. Programs Biomed. 47, 51–71.

Warfield, S., Talos, F., Tei, A., Bharatha, A., Nabavi, A., Ferrant, M., Black, P.M., Jolesz, F.A., Kikinis, R., 2002. real-time registration of volumetric brain MRI by biomechanical simulation of deformation during image guided neurosurgery. Comput. Visualization Sci. 5, 3–11.

Wendland, H., 1998. Error estimates for interpolation by compactly supported radial basis functions of minimal degree. J. Approx. Theory 93, 258–272.

Xu, M., Nowinski, W.L., 2001. Talairach–Tournoux brain atlas registration using a metal forming principle-based finite element method. Med. Image Anal. 5 (4), 271–279.